Advances in Applied Mathematics and Mechanics
Adv. Appl. Math. Mech., Vol. **3**, No. 6, pp. 759-773

DOI: 10.4208/aamm.10-m1052
December 2011

A Simplified Neuronal Model for the Instigation and Propagation of Cortical Spreading Depression

Huaxiong Huang[1,2,*], Robert M. Miura[2,3] and Wei Yao[4]

[1] *Department of Mathematics and Statistics, York University, Toronto, Ontario M3J 1P3, Canada*
[2] *Center for Applied Mathematics and Statistics, New Jersey Institute of Technology, Newark, NJ 07102, USA*
[3] *Department of Mathematical Sciences, New Jersey Institute of Technology, Newark, NJ 07102, USA*
[4] *Department of Mechanics and Engineering Science, Fudan University, Shanghai 200433, China*

Received 27 August 2010; Accepted (in revised version) 17 May 2011

Available online 31 October 2011

Abstract. In this paper, we construct a simplified neuronal model that is capable of simulating the instigation of cortical spreading depression (CSD) and propagation of a CSD wave. Our model is a simplification and extension of a single neuron model proposed in the literature for studying the instigation of CSD. Using the simplified neuronal model, we construct a network of these simplified neurons. This network model shows that the propagation of a CSD wave occurs naturally after it is instigated electrically or chemically. Although the model is simple, the speed of the CSD wave predicted by our model is consistent with experimentally observed values. Finally, our model allows us to investigate the effects of specific ion channels on the spread of a CSD wave.

AMS subject classifications: 34A33, 34A34, 92C20, 92C42, 97M60

Key words: Cortical spreading depression, neuronal model, network, numerical simulation.

1 Introduction

Cortical spreading depression (CSD) is a slow wave phenomenon in the cortex of the brain that is associated with the spread of depression of the electroencephalogram signal. Functionally, it is associated with migraine with aura, see Hadjikhane et al. [5]. CSD was discovered in 1944 by A. A. P. Leão [11], a Brazilian neurophysiologist, during his Ph.D. studies on epilepsy at the Harvard Medical School. These waves are

*Corresponding author.
URL: www.math.yorku.ca/∼hhuang
Email: hhuang@yorku.ca (H. X. Huang), miura@njit.edu (R. M. Miura), weiyao@fudan.edu.cn (W. Yao)

characterized by their slow speeds (on the order of 1 to 10 mm/min) and their appearance in a variety of cortex structures in the brains of many different animals, see Bures et al. [2], and in humans. Although CSD was discovered over 65 years ago, we still do not have a good understanding of how the different mechanisms conspire to form this coherent phenomenon [12].

While there are many interesting aspects of CSD, its intimate connection with migraine with aura makes it a particularly important neurophysiological phenomenon to try to understand from the clinical point of view. In particular, the fact that migraine occurs three times more often in women than in men and recent experimental findings by Brennan et al. [3] that show the threshold for CSD in female mice is lower than that for male mice make a compelling argument for further theoretical studies of CSD. An important question is whether we can identify physiological and/or anatomical indicators that would explain these important findings.

Mathematical models of CSD have been proposed almost since the time that CSD was discovered. The cellular automata method developed by Wiener and Rosenblueth [21] for the study of cardiac waves was used by Shibata and Bures [16] to study CSD. It was postulated early on by Grafstein [4] that potassium was the major ion involved in CSD and that repeated neuronal firings were responsible for the large increase in extracellular potassium. Hodgkin proposed a simple single partial differential equation model, essentially the first equation in the FitzHugh-Nagumo equations [13] for action potentials, to describe the leading edge of the CSD wave. Both the cellular automata methods and the simple single PDE model do not lend themselves easily to the incorporation of physiological mechanisms to explain the instigation and propagation of CSD waves. Furthermore, the flexibility in using mathematical models based on physiological mechanisms allows us to perform extensive studies of CSD occurrence which would be impossible to perform in the laboratory.

The first detailed mathematical model of CSD that incorporated physiological mechanisms was proposed by Tuckwell and Miura [20]. Their model was based on the neurotransmitter hypothesis. It had been shown by Sugaya et al. [18] that CSD waves initiated in untreated cortical tissue could propagate through TTX-treated tissue, so that CSD waves did not need action potentials for their propagation. Tuckwell and Miura [20] postulated that CSD waves could be initiated in TTX-treated tissue by application of KCl. They conjectured that a high concentration of extracellular potassium, $[K]_e$, would be sufficient to instigate a CSD wave. Since the space scale of a CSD wave is large compared to neuron size, Tuckwell and Miura formulated a one-dimensional continuum model of these processes by dividing the space into a connected extracellular space overlapping a disconnected intracellular space. The effect of this assumption is that ion diffusion can occur in the extracellular space, but cannot occur in the intracellular space, i.e., intracellular ions would first have to pass through the neuronal membrane and become an extracellular ion before it could diffuse. The model formulated by Tuckwell and Miura consists of a coupled system of nonlinear diffusion equations for the extra- and intracellular concentrations of potassium and calcium and accounts for ion movements across neuronal membranes.

In 2000, Kager et al. [7] investigated the instigation of CSD in a single neuron model by using NEURON, a modeling and computational simulation software. By focusing on sodium and potassium, two of the main ions, and ten different ion channels, their simulations produced CSD-like membrane depolarizations when stimulated by cross-membrane currents that lasted hundreds of milliseconds. Their model consisted of representing the neuron by many compartments that corresponded to the morphological structure of the soma and the spatially complex, apical and basal dendritic branches. In 2002, Kager et al. [8] followed up their 2000 study by adding chloride and similar results were obtained. Shapiro [15] proposed a continuum model for the spreading of CSD. His model differs from that of Tuckwell and Miura [20] in several aspects. First of all, Shapiro's model assumes that the neurons are connected by gap junctions, which provide bridges across which the membrane potential can propagate from one neuron to the next one. Second, he also incorporated cellular volume changes and concluded that the spreading of CSD occurs only when cells are allowed to swell. In a recent paper [1], it was proposed that the glial cells and glutamate may be responsible for the propagation of CSD based on some new experimental observations.

While several of the models proposed so far have been successful in providing a number of insights into the propagation of CSD waves, they do not answer two crucial questions: 1) what is the main mechanism responsible for the spreading of CSD, and 2) is the spreading of a CSD wave related to its instigation? In this paper, we focus on the second question. First, we construct a simplified single-neuron model that consists of the main characteristics of the more complicated model in Kager et al. [7]. The main objective is to find out if our model can mimic the behavior of the full NEURON model, i.e., the instigation of the CSD wave. In the second step, we extend the single-neuron model to a network of neurons which are coupled by diffusion to investigate the instigation and propagation of a CSD wave. In particular, we will explore the effects of several ion channels on the instigation and spreading of CSD.

The rest of the paper is organized as follows. In Section 2, a simplified neuronal model is introduced, and it is shown that the basic features of the more complicated NEURON model [7] can be reproduced and the CSD-like depolarization occurs after a membrane current is applied over a short time period. In Section 3, a network of neurons is constructed by placing the simplified neurons in a one-dimensional array. The extracellular space (ECS) is assumed to be connected and ions can diffuse freely in the ECS. It is shown that when the membrane current is applied to several neurons simultaneously, they become depolarized as in the single neuron case. Furthermore, the ECS concentration of potassium outside the neighboring neurons is due to molecular diffusion, which induces the firing of these neighboring neurons. These neurons undergo depolarization one-by-one, generating CSD. In particular, it was found experimentally [12] that action potentials are not necessary to generate CSD. By disabling the fast transient sodium channel, we are able to show that CSD can be instigated and subsequent spreading can occur without action potentials. In Section 4, the role of NMDA channels in the instigation and propagation of CSD is also investigated. In

Section 5, we complete the paper with a brief summary and a discussion of future directions.

2 Single neuron: a simplified model

Our first model of the neuron consists only of the soma[†], which is assumed to be spatially homogeneous. Following Kager et al. [7], we consider only the two ions, sodium Na and potassium K, with intra- and extracellular concentrations denoted by $[ion]_i$ and $[ion]_e$ (mM), respectively, where $ion =$ Na and K. We consider only two compartments that represent the intra- and extracellular spaces. The membrane potential E_m (mV) is governed by the ordinary differential equation

$$C_m \frac{dE_m}{dt} = -I, \tag{2.1}$$

where C_m is the membrane capacitance per unit surface area (farad/cm^2) and I is the total cross-membrane ionic current per unit surface area (mA/cm^2).

We assume that the membrane currents in the soma used by Kager et al. [7] apply here. The total cross-membrane current in the soma is given by the sum of the sodium currents, $I_{Na} = I_{Na,T} + I_{Na,P} + I_{Na,Leak} + I_{Na,Pump}$, the potassium currents, $I_K = I_{K,DR} + I_{K,A} + I_{K,Leak} + I_{K,Pump}$, the leak current, I_{Leak}, and the sodium-potassium exchange pump currents, $I_{Na,Pump}$ and $I_{K,Pump}$[‡]. An additional stimulus current, I_{Sti}, can be included to trigger CSD. The cross-membrane currents are modeled using: 1) the Goldman-Hodgkin-Katz (GHK) formulas for the active membrane currents, namely, the fast transient sodium current, $I_{Na,T}$, the persistent sodium current, $I_{Na,P}$, the potassium delayed rectifier current, $I_{K,DR}$, and the transient potassium current, $I_{K,A}$; and 2) the Hodgkin-Huxley (HH) model for the leak currents, namely, the sodium leak current, $I_{Na,Leak}$, the potassium leak current, $I_{K,Leak}$, and the fixed leak current, I_{Leak}. The GHK current is suitable when there is a large difference in concentrations in the ICS and ECS compartments, as argued by Koch and Segev [9].

The general expressions for the GHK and HH types of currents are given by

$$I_{ion,GHK} = m^p h^q \frac{g_{ion,GHK} F E_m \Big([ion]_i - \exp\Big(-\frac{E_m}{\phi} \Big) [ion]_e \Big)}{\phi \Big(1 - \exp\Big(-\frac{E_m}{\phi} \Big) \Big)}, \tag{2.2a}$$

$$I_{ion,HH} = g_{ion,HH} \big(E_m - E_{ion} \big), \tag{2.2b}$$

where $g_{ion,GHK}$ and $g_{ion,HH}$ are the conductances for $ion =$ Na and K, and m and h are the activation and inactivation gating variables, respectively, for the different GHK-modeled channels that are ion-specific. Note that the $g_{ion,HH}$ conductances for the

[†]The dendrite will be included later in Section 4 as an additional compartment.

[‡]In the dendrite (as in Section 4), the NMDA currents, $I_{Na,NMDA}$ and $I_{K,NMDA}$, are added to the total current and the $I_{Na,T}$ current is removed.

leak currents are assumed to be constant. The parameter $\phi = RT/F$, where R is the universal gas constant, T is the absolute temperature, and F is the Faraday constant. Finally, E_{ion} is the Nernst potential for $ion =$ Na and K given by

$$E_{ion} = \phi \log \frac{[ion]_e}{[ion]_i}. \tag{2.3}$$

In addition to the ion-specific leak currents, there is a general leak current given by

$$I_{Leak} = g_{HH}(E_m + 70), \tag{2.4}$$

where g_{HH} is a constant conductance. This current drives the membrane potential towards a rest state of -70 mV. The pump currents are given by $I_{Na,Pump} = 3I_{Pump}$ and $I_{K,Pump} = -2I_{Pump}$ [10] where

$$I_{Pump} = \frac{I_{\max}}{\left(1 + 1.75[K]_e^{-1}\right)^2 \left(1 + 5[Na]_i^{-1}\right)^3}. \tag{2.5}$$

We have adjusted the constants given in [10] in order to maintain the ion concentrations and membrane potential in the cortex at the rest state.

The time evolution of the concentrations of potassium and sodium ions are determined by the cross-membrane currents as follows

$$\frac{d[Na]_i}{dt} = -\frac{S}{FV_i} I_{Na}, \tag{2.6a}$$

$$\frac{d[Na]_e}{dt} = \frac{S}{FV_e} I_{Na}, \tag{2.6b}$$

$$\frac{d[K]_i}{dt} = -\frac{S}{FV_i} I_K, \tag{2.6c}$$

$$\frac{d[K]_e}{dt} = \frac{S}{FV_e} I_K, \tag{2.6d}$$

where S, V_i, and V_e are the soma surface area and intra- and extracellular volumes, respectively.

The gating variables, m and h, satisfy the following equations

$$\frac{dm}{dt} = \alpha_m(1 - m) - \beta_m m, \tag{2.7a}$$

$$\frac{dh}{dt} = \alpha_h(1 - h) - \beta_h h, \tag{2.7b}$$

and the values of α and β are given in Table 1, along with the exponents p and q [7]. The extracellular volume is assumed to be 15% of the intracellular value, i.e., $V_e = 0.15\, V_i$. Other relevant parameter values are: $R = 8.31$ (mV coulomb/mmol K) and $F = 96.485$ coulomb/mM. Finally, we note that the ion concentrations are conventionally measured in mM, while in Eqs. (2.6a)-(2.6d), the specified length unit used is cm. Thus, a scale factor of 10^{-3} needs to multiply the right-hand sides of Eqs. (2.6a)-(2.6d).

Table 1: Parameter values for active membrane ionic currents, from [7, 8].

Currents mA/cm^2	$g_{ion,GHK}$ S/cm^2	Gates $m^p h^q$	Voltage-Dependent Rate Constants
$I_{Na,T}$	100×10^{-5}	$m^3 h$	$\alpha_m = 0.32 \frac{E_m+51.9}{1-\exp[-(0.25E_m+12.975)]}$ $\beta_m = 0.28 \frac{E_m+24.89}{\exp[0.2E_m+4.978)]-1}$ $\alpha_h = 0.128 \exp[-(0.056E_m + 2.94)]$ $\beta_h = \frac{4}{1+\exp[-(0.2E_m+6)]}$
$I_{Na,P}$	2×10^{-5}	$m^2 h$	$\alpha_m = \frac{1}{6(1+\exp[-(0.143E_m+5.67)])}$ $\beta_m = \frac{\exp[-(0.143E_m+5.67)]}{6(1+\exp[-(0.143E_m+5.67)])}$ $\alpha_h = 5.12 \times 10^{-8} \exp[-(0.056E_m + 2.94)]$ $\beta_h = \frac{1.6\times10^{-6}}{1+\exp[-(0.2E_m+8]}$
$I_{K,DR}$	100×10^{-5}	m^2	$\alpha_m = 0.016 \frac{E_m+34.9}{1-\exp[-(0.2E_m+6.98)]}$ $\beta_m = 0.25 \exp[-(0.25E_m + 1.25)]$
$I_{K,A}$	10×10^{-5}	$m^2 h$	$\alpha_m = 0.02 \frac{E_m+56.9}{1-\exp[-(0.1E_m+5.69)]}$ $\beta_m = 0.0175 \frac{E_m+29.9}{\exp(0.1E_m+2.99)-1}$ $\alpha_h = 0.016 \exp[-(0.056E_m + 4.61)]$ $\beta_h = \frac{0.5}{1+\exp[-(0.2E_m+11.98)]}$
I_{NMDA}	10×10^{-5}	mh	$\alpha_m = \frac{0.5}{1+\exp[\frac{13.5-[K]e}{1.42}]}$ $\beta_m = 0.5 - \alpha_m$ $\alpha_h = \frac{1}{2000\left(1+\exp[\frac{[K]e-6.75}{0.71}]\right)}$ $\beta_h = 5 \times 10^{-4} - \alpha_h$

The initial resting ion concentrations consistent with those in [7, 8] are obtained by modifying the sodium-potassium exchange pump function and running the model equations until a steady state is reached. These values are given in Table 2 together with other parameter values.

Following Kager et al. [7], we apply an electrical current stimulus to the soma for 200 ms. The results are shown in Fig. 1 with time axis up to 30ms, where it can be seen in Fig. 1(a) that the electrical current stimulus produces action potentials with a depolarizing base that lasts for about 100ms, after which there is a CSD-like time course, i.e., sustained membrane depolarization even after the stimulus is withdrawn. With the electrical current stimulus and the removal of the fast transient sodium current, $I_{Na,T}$, there are no action potentials as shown in Fig. 1(c). The corresponding extra- and intracellular ion concentrations of potassium (blue solid and dashed lines, respectively) and sodium (red solid and dashed lines, respectively) for these two cases can be seen in Figs. 1(b) and (d).

CSD can also be triggered by other types of stimuli, e.g., application of KCl at the initial time, which occurs in the model as initial data for potassium. In Fig. 2 with

Table 2: Initial resting values and other relevant parameter values for the computations, following [7, 8].

Parameter	Value	Unit
d_S (diameter of soma)	5.45×10^{-4}	cm
A_S (surface of soma)	1586×10^{-8}	cm^2
V_S (volume of soma)	2160×10^{-12}	cm^3
C_m(membrane capacitance)	7.5×10^{-7}	$s/\Omega\ cm^2$
$I_{\max}$	0.013	mA/cm^2
E_m	-70	mV
$[K]_e$	3.5	mM
$[K]_i$	133.5	mM
$[Na]_e$	140	mM
$[Na]_i$	10	mM
$m_{Na,T,0}$ (initial value of m for $I_{Na,T}$)	5×10^{-3}	
h_{T0} (initial value of h for $I_{Na,T}$)	0.995	
m_{P0} (initial value of m for $I_{Na,P}$)	1.3×10^{-2}	
m_{KDR0} (initial value of m for $I_{K,DR}$)	1.3×10^{-3}	
m_{KA0} (initial value of m for $I_{K,A}$)	0.12	
h_{KA0} (initial value of h for $I_{K,A}$)	0.12	

time axis up to 30 sec, we compare the results when the two instigation methods are used, namely, when an electrical current stimulus is applied for 200 ms with the fast transient sodium current, $I_{Na,T}$, activated in Fig. 2(a), and when KCl is applied with no fast transient sodium current activated in Fig. 2(b). It can be seen that in both cases, the membrane potential depolarizes and eventually repolarizes. The difference in the time that the membrane remains depolarized is likely due to the fast transient sodium current where there is delayed repolarization.

3 Small networks of simplified point neuron models

In the previous section, we established that a simplified neuron model can produce CSD-like membrane potential behavior when it is stimulated with an electrical current. Here, we will investigate the spreading of a CSD-like wave by considering a network of a finite number of these simplified neuron models, immersed in an extracellular space.

3.1 Small network model

In contrast to the previous section where the ions remain in the ECS next to the neuron, we assume that the ions can diffuse within the ECS, but there is no diffusion in the ICS. In other words, we assign an index j to each neuron and the associated extracellular space, and denote the intra- and extracellular concentrations of the ions by $[ion]_{i,j}$ and $[ion]_{e,j}$, respectively. In addition, we assume that the extracellular concentration $[ion]_{e,j}$ varies, and that it "flows" from higher concentration to lower values. Therefore, we

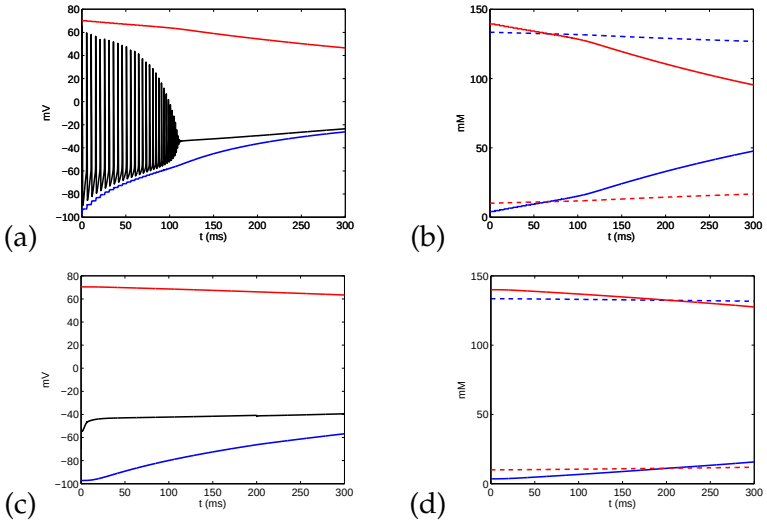

Figure 1: Time courses (300 ms) of the membrane potential (black) and Nernst potentials for potassium (blue) and sodium (red) with 200 ms electrical stimulation: (a) with $I_{Na,T}$ producing action potentials and depolarization; and (c) without $I_{Na,T}$ and producing no action potentials. Also plotted are the corresponding extra- and intracellular concentrations of potassium (blue solid and dashed lines, respectively) and sodium (red solid and dashed lines, respectively), (b) with $I_{Na,T}$, and (d) without $I_{Na,T}$. Even though the propagation of the depolarization cannot be produced using a single neuron, the change of membrane potential and the massive redistribution of ion concentrations are similar to the phenomena observed during a CSD wave. These will be referred to as CSD-like time courses in the rest of the paper, following [7].

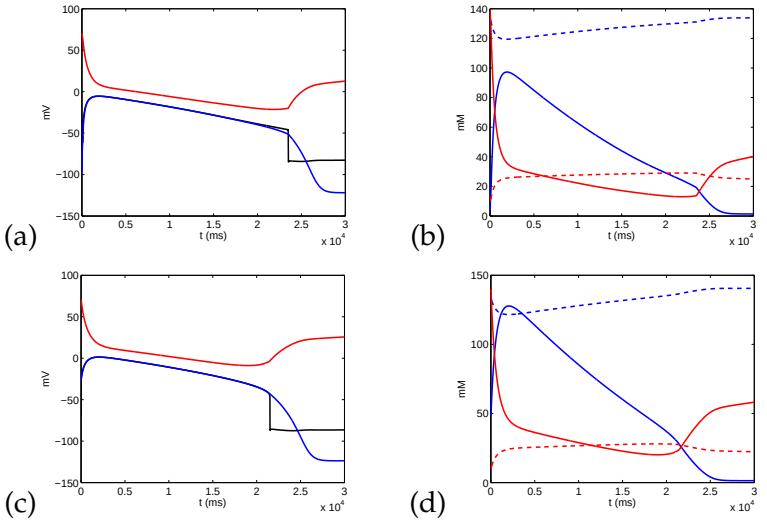

Figure 2: CSD-like time courses (30 seconds) of the membrane potential (black) and Nernst potentials for potassium (blue) and sodium (red): (a) instigation using electric current with $I_{Na,T}$ active, and (c) instigation by the application of KCl without $I_{Na,T}$. It can be seen that the behaviors of the membrane potential and other quantities are similar except the recovery is sooner when the fast transient sodium current is not present. Also plotted are the corresponding extra- and intracellular ion concentrations of potassium (blue solid and dashed lines, respectively) and sodium (red solid and dashed lines, respectively), (b) with $I_{Na,T}$, and (d) without $I_{Na,T}$.

replace the Eqs. (2.6b) and (2.6d) by

$$\frac{d[Na]_{e,j}}{dt} = \frac{S}{FV_e} I_{Na,j} + \gamma_{Na}\big([Na]_{e,j+1} + [Na]_{e,j-1} - 2[Na]_{e,j}\big), \tag{3.1a}$$

$$\frac{d[K]_{e,j}}{dt} = \frac{S}{FV_e} I_{K,j} + \gamma_{K}\big([K]_{e,j+1} + [K]_{e,j-1} - 2[K]_{e,j}\big), \tag{3.1b}$$

for neuron j and the extracellular space associated with it. Here, γ_{Na} and γ_K are coefficients that are obtained from the molecular diffusion coefficients, D_{Na} and D_K, scaled by the square of the average distance (δ) between the neurons. In other words, we compute $\gamma_{ion} = D_{ion}/\delta^2$, where $D_{Na} = 1.33 \times 10^{-5}$ cm^2/s and $D_K = 1.96 \times 10^{-5}$ cm^2/s [14]. For the intracellular concentrations, the Eqs. (2.6a) and (2.6c) are unchanged except for the additional index

$$\frac{d[Na]_{i,j}}{dt} = -\frac{S}{FV_i} I_{Na,j}, \tag{3.2a}$$

$$\frac{d[K]_{i,j}}{dt} = -\frac{S}{FV_i} I_{K,j}. \tag{3.2b}$$

In the brain-cell microenvironment, glial cells occupy an amount of space similar to that of neurons; therefore, we have experimented with two extreme cases where the distances between neurons are equal to: 1) the soma diameter, and 2) twice the soma diameter. In both cases, we obtained similar results. Here we present only the results where the distance between the neurons is equal to the soma diameter. When a current stimulus is injected into the first neuron for 200 ms, it triggers action potentials. However, at the end of the stimulation, the membrane potential returns to its rest value, see Fig. 3(a), and the other neurons remain depolarized, as shown. In this case, the extracellular potassium concentration outside the stimulated neuron is unable to build up to a critical value because of ion diffusion to the extracellular spaces of neighboring neurons, cf. Fig. 3(b). Although the identification of this critical value of the ECS potassium concentration is of mathematical interest, our main objective in this study is to provide a qualitative understanding of the instigation and propagation of CSD waves. Therefore, this is left as a topic for further study. When we apply an identical current stimulus for 200 ms to three neurons, all three neurons depolarize after a prolonged period of action potentials, which trigger significant buildup of the extracellular potassium concentration and influx of sodium ions. As a consequence of the diffusion of extracellular potassium to the extracellular spaces of neighboring neurons, action potentials are induced in neighboring neurons, resulting in a cascade of depolarization of neuronal membrane potentials one after the other, a spreading of CSD-like depolarization, cf. Fig. 4.

Another stimulus for CSD waves is the application of KCl, as in Fig. 5 where we plot the membrane potential and the ECS potassium concentration of individual neurons from the time of application of KCl up to 400 ms. The application of KCl is assumed to be confined to the ECS of the first three neurons. While the first three

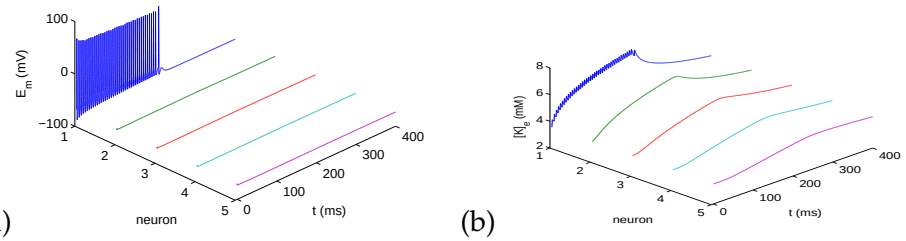

(a) (b)

Figure 3: Time courses of the membrane potential and extracellular concentrations of potassium when the first neuron is stimulated by an electrical current. (a) Membrane potentials of individual neurons. (b) Concentrations near potassium in the ECS of neurons. The neuron being stimulated fires and the corresponding ECS potassium increases in an oscillatory fashion due to the effect of the action potentials. ECS concentration of the neighboring neurons also increases due to diffusion in the ECS. However, the increases are smaller and smoother as one moves away from the stimulated neurons. Depolarization of the membrane potential does not propagate to the neighboring neurons.

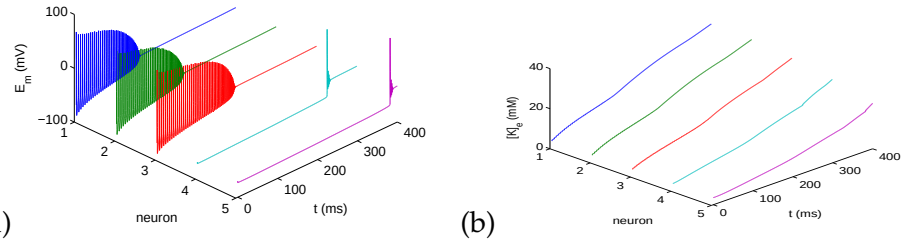

(a) (b)

Figure 4: Time courses of the membrane potential (a) and extracellular concentrations of potassium (b) when the first three neurons are stimulated by electrical currents. CSD is triggered as the other neurons start firing and the corresponding ECS potassium concentration builds up.

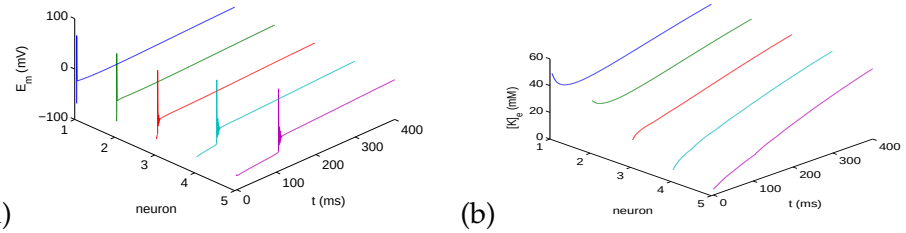

(a) (b)

Figure 5: Time courses of the membrane potential (a) and extracellular concentrations of potassium (b) when KCl is injected into the ECS of the first three neurons. Spreading of depolarization among neurons is apparent.

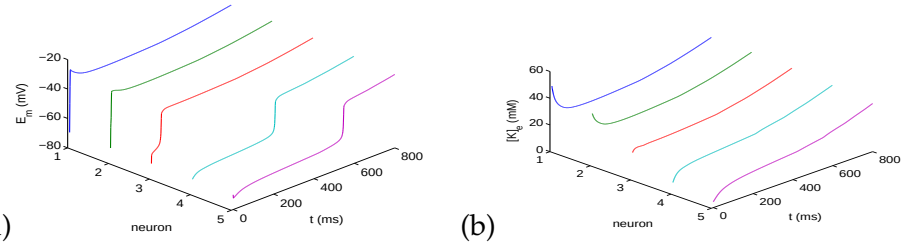

(a) (b)

Figure 6: Time courses of the membrane potential (a) and extracellular concentrations of potassium (b) when KCl is injected into the ECS of the first three neurons with the fast transient sodium current disabled. Spreading of CSD occurs without the action potentials.

neurons (only the third neuron is plotted) are depolarized almost instantly after the injection of KCl, the other neurons initiate the firing of acting potentials and undergo depolarization one-by-one, as shown in Fig. 5, which is similar to the case when an electrical current stimulus is applied.

As noted earlier, it has been observed experimentally that CSD can be generated even without action potentials, i.e., by blocking the fast transient sodium current, $I_{Na,T}$, and we also have demonstrated this in our model in Section 2.

3.2 Spreading depolarization and increasing potassium concentration

We now explore the spreading of the membrane depolarization by application of KCl when $I_{Na,T}$ has been removed. In Fig. 6, we plot the membrane potential and the ECS potassium concentration from the time of application of KCl up to 800 ms. The application of KCl is assumed to be confined to the ECS of the first three neurons. While the first three neurons (only the third neuron is plotted) are depolarized almost instantly after the application of KCl, the other neurons undergo depolarization one-by-one, without the firing of action potentials, as shown in Fig. 6. An important feature of a model is its ability to make quantitative predictions. Therefore, we have computed the propagation speed of the CSD wave and found that it travels at approximately 8 and 4 mm/min when the fast transient sodium channels are included and removed, respectively. Both are within the range of experimentally observed values.

4 Effect of NMDA currents

The roles of NMDA currents and glutamate have been discussed extensively in [12,17]. While it is evident that they do play a role in CSD, it is not clear if the activation of NMDA receptors is absolutely required for the generation of SD [17]. On the other hand, it has been pointed out by Takano et al. [19] that in some cases, blocking the NMDA receptors prevents the instigation of CSD but not its propagation once it has started. In this section, we extend our model to investigate the role of NMDA currents. Since the NMDA currents only occur in dendrites, we include the dendrites in our model by adding another compartment. The functional form of the NMDA current is given in Table 1. Then we modify the extracellular ion concentration equations as follows:

$$\frac{d[Na]^S_{e,j}}{dt} = \frac{S^S I^S_{Na,j}}{FV^S_e} + \beta_{Na}\big([Na]^D_{e,j} - [Na]^S_{e,j}\big) + \gamma_{Na}\big([Na]_{e,j+1} + [Na]_{e,j-1} - 2[Na]_{e,j}\big), \quad (4.1a)$$

$$\frac{d[K]^S_{e,j}}{dt} = \frac{S^S I^S_{K,j}}{FV^S_e} + \beta_K\big([K]^D_{e,j} - [K]^S_{e,j}\big) + \gamma_K\big([K]_{e,j+1} + [K]_{e,j-1} - 2[K]_{e,j}\big), \quad (4.1b)$$

$$\frac{d[Na]^D_{e,j}}{dt} = \frac{S^D I^D_{Na,j}}{FV^D_e} + \beta_{Na}\big([Na]^S_{e,j} - [Na]^D_{e,j}\big) + \gamma_{Na}\big([Na]_{e,j+1} + [Na]_{e,j-1} - 2[Na]_{e,j}\big), \quad (4.1c)$$

$$\frac{d[K]_{e,j}}{dt} = \frac{S^D I^D_{K,j}}{FV^D_e} + \beta_K\big([K]^S_{e,j} - [K]^D_{e,j}\big) + \gamma_K\big([K]_{e,j+1} + [K]_{e,j-1} - 2[K]_{e,j}\big), \quad (4.1d)$$

where the superscripts S and D denote soma and dendrite, respectively. The intracellular ion concentration equations are changed to

$$\frac{d[Na]^S_{i,j}}{dt} = -\frac{S^S}{FV^S_i} I^S_{Na,j} + \beta_{Na}\big([Na]^D_{i,j} - [Na]^S_{i,j}\big), \tag{4.2a}$$

$$\frac{d[K]^S_{i,j}}{dt} = -\frac{S^S}{FV^S_i} I^S_{K,j} + \beta_K\big([K]^D_{i,j} - [K]^S_{i,j}\big), \tag{4.2b}$$

$$\frac{d[Na]^D_{i,j}}{dt} = -\frac{S^D}{FV^D_i} I^D_{Na,j} + \beta_{Na}\big([Na]^S_{i,j} - [Na]^D_{i,j}\big), \tag{4.2c}$$

$$\frac{d[K]^D_{i,j}}{dt} = -\frac{S^D}{FV^D_i} I^D_{K,j} + \beta_K\big([K]^S_{i,j} - [K]^D_{i,j}\big), \tag{4.2d}$$

and the equations for the membrane potentials in the soma and dendrite become

$$C_m \frac{dE^S_m}{dt} = -I^S + \beta_E(E^D_m - E^S_m), \quad C_m \frac{dE^D_m}{dt} = -I^D + \beta_E(E^S_m - E^D_m). \tag{4.3}$$

The parameters are given by $\beta_{Na} = 2D_{Na}/\delta^2_D$, $\beta_K = 2D_K/\delta^2_D$, $\beta_E = 2D/\delta^2_D$, and δ_D is the half length of the effective dendritic tree, estimated at 4.5×10^{-2} cm [6].

In Fig. 7, we plot the time courses of the soma membrane potential and extracellular potassium concentration when the model includes both the soma and dendrite. It can be seen that the characteristics of these curves do not change substantially from those for the soma alone. Once a wave of CSD has been instigated, it propagates similarly in the two models, without and with the dendrite. On the other hand, blocking the NMDA channels, prevents CSD instigation, as shown by Fig. 8.

Most interestingly, if we block the NMDA channels in the regions away from where KCl is applied, then the CSD wave is not blocked. It passes right through the neurons whose NMDA channels are blocked, cf. Fig. 9, with some changes in the level of depolarizations in the soma. These results indicate that the instigation and spreading of membrane depolarization could be affected differently by blocking the NMDA channels. Even though the detailed mechanisms that affect the NMDA channels are not modeled here, our model is still capable of producing interesting phenomena that can be further explored by a more comprehensive study, either experimentally or using mathematical modeling.

5 Discussion and conclusions

In this paper, we have developed a simplified neuronal model of cortical spreading depression (CSD), which is computationally much more efficient than using the program NEURON. We have shown with our model for a single neuron that a CSD-like depolarization can be instigated with an electrical current stimulus. This allows us to construct a network of neurons that can be used to investigate the spreading of CSD-like membrane depolarization. We have carried out numerical simulations using the

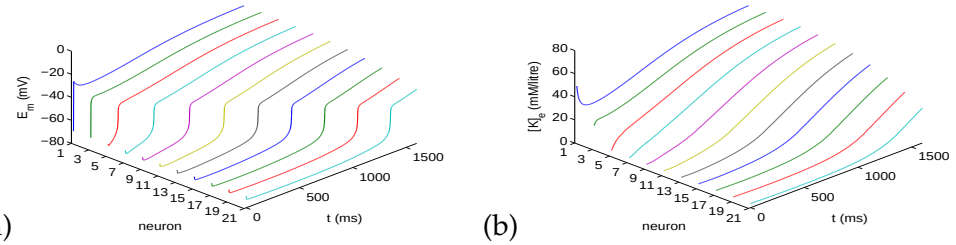

Figure 7: Time courses of the soma membrane potential (a) and the corresponding extracellular concentration of potassium (b) when KCl is injected into the ECS of the first three neurons with the fast transient sodium current disabled. Here we have included dendrites as a second compartment with NMDA currents.

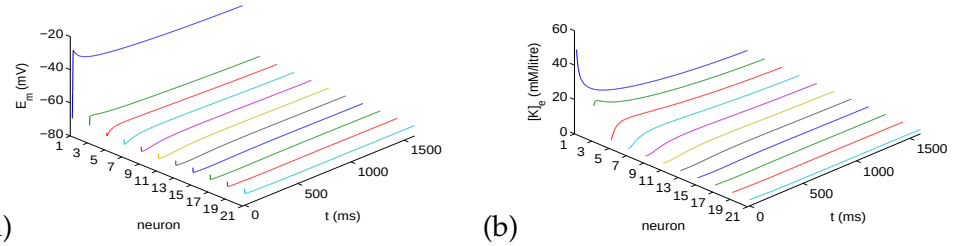

Figure 8: Same as Fig. 7 except that there are no NMDA currents. Depolarization of membrane potential does not propagate into neighboring neurons.

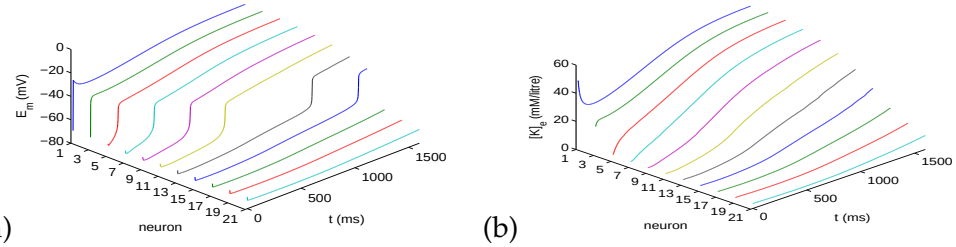

Figure 9: Same as Fig. 7 except that there are no NMDA currents from the 10th neuron and beyond. Depolarization of membrane potential is delayed but is not stopped by the blocking of NMDA currents.

simplified single neuron model and a network of simplified neurons with results that illustrate CSD depolarization and wave propagation using either an electrical current stimulus or an application of KCl in the extracellular space. Furthermore, CSD can be instigated and propagated even with the fast transient sodium channel blocked, i.e., no action potentials occur during the spreading of CSD. In addition, blocking the NMDA channels prevents the instigation of CSD, but does not stop it, if CSD has already been instigated.

Previous models for the propagation of CSD included extracellular diffusion of ions, and special mechanisms, such as neurotransmitters, gap-junctions, or cell swelling. Here our model makes no assumptions except that the ions are allowed to diffuse in the ECS. In addition, our model shows that it is not necessary to separate the instigation and spreading of CSD while blocking NMDA channels does affect the instigation and spreading differently. Finally, we point out that our basic model is developed by simplifying an earlier model proposed by Kager et al. [7]. Obviously,

other effects not included in our model could also be important in the instigation and spreading phases of CSD, and they can be incorporated into our current model. We are in the process of constructing a continuum model, which can be used to investigate the effects of additional ions (such as chloride), the change of volume fraction, cell swelling, membrane conductances, and background ion concentrations. Another step to understanding CSD is to incorporate the role of glial cells. Our model also provides a starting point for further exploration of CSD related phenomena, such as vasodilation and vasoconstriction.

Acknowledgements

We would like to thank the Natural Sciences and Engineering Research Council of Canada (H. Huang), the National Science Foundation of the United States (R. M. Miura), the Mathematics of Information Technology and Complex Systems, Centers of Excellence, Canada (H. Huang and W. Yao), and the Chinese Ministry of Education (W. Yao) for providing financial support.

References

[1] M. R. BENNETT, L. FARNELL AND W. G. GIBSON, *A quantitative model of cortical spreading depression due to purinergic and gap-junction transmission in astrocyte networks*, Biophys. J., 95 (2008), pp. 5648–5660.
[2] J. BUREŠ, O. BUREŠOVÁ AND J. KŘIVÁNEK, The Mechanism and Applications of Leao's Spreading Depression of Electroencephalographic Activity, Prague, Academia, 1974.
[3] K. C. BRENNAN, M. R. REYES, H. E. L. VALDÉS, A. P. ARNOLD AND A. C. CHARLES, *Reduced threshold for cortical spreading depression in female mice*, Ann. Neurol., 61 (2007), pp. 603–606.
[4] B. GRAFSTEIN, *Mechanism of spreading depression*, J. Neurophys., 19 (1965), pp. 154–171.
[5] N. HADJIKHANE, M. S. DEL RIO, O. WU, D. SCHWARTZ, D. BAKKER, B. FISCHI, K. K. KWONG, F. M. CUTRER, B. R. ROSEN, R. B. H. TOOTELL, A. G. SORENSEN AND M. A. MOSKOWITZ, *Mechanisms of migraine aura revealed by functional MRI in human visual cortex*, Proc. Natl. Acad. Sci., 98 (2001), pp. 4687–4692.
[6] C. V. HOWARD, L. M. CRUZ-ORIVE AND H. YAEGASHI, *Estimating neuron dendritic length in 3D from total vertical projections and from vertical slices*, Acta Neurol Scand., 137 (1990), pp. 14–19.
[7] H. KAGER, W. J. WADMAN AND G. G. SOMJEN, *Simulated seizures and spreading depression in a neuron model incorporating interstitial space and ion concentrations*, J. Neurophys., 84 (2000), pp. 495–512.
[8] H. KAGER, W. J. WADMAN AND G. G. SOMJEN, *Conditions for the triggering of spreading depression studied with computer simulations*, J. Neurophys., 88 (2002), pp. 2700–2712.
[9] C. KOCH AND I. SEGEV, Methods in Neuronal Modeling: From Ions to Networks, MIT Press, Cambridge, MA, 1998.
[10] P. LÄUGER, Electrogenic Ion Pumps, Sinauer, Sunderland MA, 1991.
[11] A. A. P. LEÃO, *Spreading depression of activity in the cerebral cortex*, J. Neurophys., 7 (1944), pp. 359–390.

[12] H. MARTINS-FERREIRA, M. NEDERGAARD AND C. NICOLSON, *Perspective on spreading depression*, Brain Res. Rev., 32 (2000), pp. 215–234.
[13] J. NAGUMO, S. ARIMOTO AND S. YOSHIZAWA, *An active pulse transmission line simulating nerve axon*, Proc. IRE, 50 (1962), pp. 2061–2070.
[14] B. E. SHAPIRO, An Elecrophysiological Model of Gap-Junction Mediated Cortical Spreading Depression Including Osmotic Volume Changes, PhD Dissertation, Biomathematics, UCLA, 2000.
[15] B. E. SHAPIRO, *Osmotic forces and gap junctions in spreading depression: a computational model*, J. Comput. Neurosci., 10 (2001), pp. 99–120.
[16] M. SHIBATA AND J. BURES, *Techniques for termination of reverberating spreading depression in rats*, J. Neurophys., 38 (1975), pp. 158.
[17] G. G. SOMJEN, *Mechanisms of spreading depression and hypoxic spreading depression-like depolarization*, Phys. Rev., 81 (2001), pp. 1065–1096.
[18] E. SUGAYA, M. TAKATO AND Y. NODA, *Neuronal and glial activity during spreading depression in cerebral cortex of cat*, J. Neurophys., 38 (1975), pp. 822–841.
[19] T. TAKANO, G. F. TIAN, W. PENG, N. LOU, D. LOVATT, A. J. HANSEN, K. A. KASISCHKE AND M. NEDERGAARD, *Cortical spreading depression causes and coincides with tissue hypoxia*, Nature Neurosci., 10 (2006), pp. 754–762.
[20] H. C. TUCKWELL AND R. M. MIURA, *A mathematical model for spreading cortical depression*, Biophys. J., 23 (1978), pp. 257–276.
[21] N. WIENER AND A. ROSENBLUETH, *The mathematical formulation of the problem of conduction of impulses in a network of connected excitable elements, specifically in cardiac muscle*, Arch. Inst. Cardiol. Mex., 16 (1946), pp. 205–265.